Soils and Foundations 2014;54(3):269–279

The Japanese Geotechnical Society

Soils and Foundations

www.sciencedirect.com
journal homepage: www.elsevier.com/locate/sandf

Building response to tunnelling ☆

Ruaidhri Farrell[a,*], Robert Mair[b], Alessandra Sciotti[c], Andrea Pigorini[c]

[a]*Laing O'Rourke, UK*
[b]*Sir Kirby Laing Professor of Civil Engineering, University of Cambridge, Cambridge, UK*
[c]*Italferr, Italy*

Received 19 July 2012; received in revised form 27 May 2013; accepted 25 August 2013
Available online 23 May 2014

Abstract

Understanding how buildings respond to tunnelling-induced ground movements is an area of great importance for urban tunnelling projects, particularly for risk management. In this paper, observations of building response to tunnelling, from both centrifuge modelling and a field study in Bologna, are used to identify mechanisms governing the soil–structure interaction. Centrifuge modelling was carried out on an 8-m-diameter beam centrifuge at Cambridge University, with buildings being modelled as highly simplified elastic and inelastic beams of varying stiffness and geometry. The Bologna case study presents the response of two different buildings to the construction of a sprayed concrete lining (SCL) tunnel, 12 m in diameter, with jet grouting and face reinforcement.

In both studies, a comparison of the building settlement and horizontal displacement profiles, with the greenfield ground movements, enables the soil structure interaction to be quantified. Encouraging agreement between the modification to the greenfield settlement profile, displayed by the buildings, and estimates made from existing predictive tools is observed. Similarly, both studies indicate that the horizontal strains, induced in the buildings, are typically at least an order of magnitude smaller than the greenfield values. This is consistent with observations in the literature. The potential modification to the settlement distortions is shown to have significant implications on the estimated level of damage. Potential issues for infrastructures connected to buildings, arising from the embedment of rigid buildings into the soil, are also highlighted.

Keywords: Soil–structure interaction; Tunnels; Building response; Centrifuge modeling; Case history; Settlements

1. Introduction

While relatively accurate predictions of the 'greenfield' ground movements due to tunnelling, in both vertical and horizontal planes, can be made (Mair and Taylor, 1997), the presence of a structure may alter these movements by what is termed 'soil–structure interaction'. The estimation of the risk of damage to buildings, however, typically involves assuming that the structure deforms according to the greenfield ground movements, i.e., fully flexibly, and ignoring the stiffness of the building (e.g., Mair et al., 1996). Estimates of the damage using this assumption can be highly conservative.

☆Geotechnical classification categories: E12 Soil–structure interaction. H05 Tunnels and underground openings.

*Corresponding author. Tel.: +447942571535.
E-mail address: farrelrp@gmail.com (R. Farrell).

Peer review under responsibility of The Japanese Geotechnical Society.

Production and hosting by Elsevier

http://dx.doi.org/10.1016/j.sandf.2014.04.003
0038-0806/

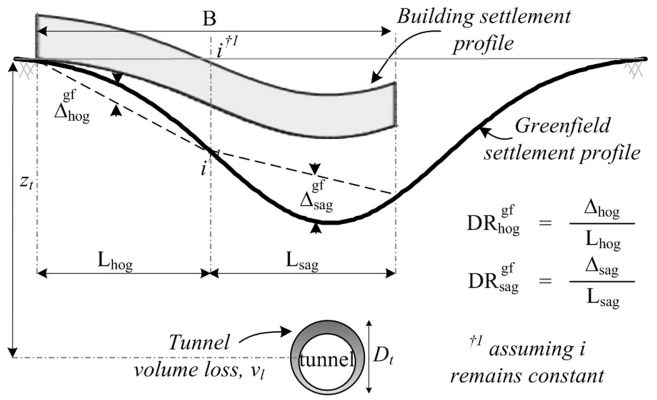

Fig. 1. Influence of soil–structure interaction on settlement distortions Aerial view of site and tunnelling works.

Potts and Addenbrooke (1997) conducted a parametric finite element analysis to investigate the response of buildings to tunnelling. Two parameters were defined to characterise the modification to the settlement and the axial response of buildings; they were the relative bending stiffness (ρ^*) and the relative axial stiffness (α^*). ρ^* and α^* were later modified by Franzius et al. (2006), the former to be dimensionless. Expressions for ρ^*_{mod} and α^*_{mod}, defined by Franzius et al. (2006), are presented in Eqs. 1 and 2, respectively.

$$\rho^*_{mod} = \frac{EI}{E_s B^2 z_0 L} \tag{1}$$

$$\alpha^*_{mod} = \frac{EA}{E_s BL} \tag{2}$$

where EI and EA are the bending stiffness and the axial stiffness of the structure, respectively. E_s is the secant stiffness of the soil at an axial strain of 0.01% and at a depth of $z=z_0/2$. B is the building width and L is the length parallel to the tunnel heading. The dimensions are illustrated in Fig. 1.

Settlement distortions to buildings are typically measured in both hogging and sagging modes of deformation using the deflection ratio (Δ/L or DR, defined in Fig. 1). The hogging and sagging regions are partitioned by the point of inflexion (i) of the settlement trough, assuming that each building responds fully flexibly. Potts and Addenbrooke (1997) quantified the modification to settlement distortions in terms of the ratio of the measured deflection ratio to the equivalent greenfield value, as presented in Eq. (3). This ratio is given the term 'modification factor' (M^{DRhog} and M^{DRsag}).

$$M^{DR} = \frac{DR^{str}}{DR^{GF}} \tag{3}$$

where DR^{GF} is the greenfield deflection ratio and DR^{str} is the deflection ratio displayed by the building; both are defined separately in hogging and sagging.

Modification factors to the greenfield settlement distortions are highly dependent on ρ^*_{mod} (Franzius et al., 2006). Similarly, the modification to tensile and compressive horizontal strains, in the hogging and sagging regions, respectively, are highly dependent on α^*_{mod} (Franzius et al., 2006).

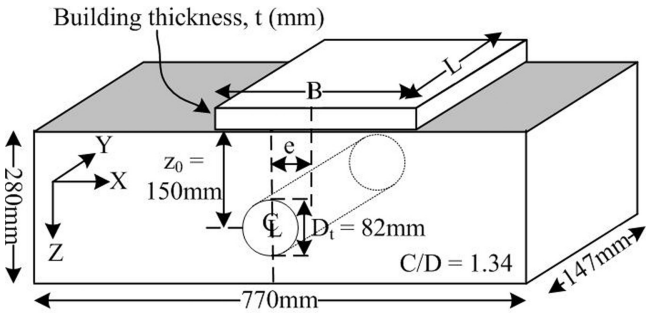

Fig. 2. Model dimensions (in model scale).

This paper presents the results of a series of centrifuge tests in which idealised model buildings in the form of beam structures, of varying stiffness and geometry, are subjected to tunnelling-induced ground movements. Mechanisms governing the effects of the soil–structure interaction are identified and compared with observations from a case study of a tunnelling project in Bologna, in which the response of two buildings, of significantly different stiffness, were extensively monitored. Based on these observations, methods commonly used to assess the risk of damage to buildings from tunnelling are discussed.

2. Centrifuge modelling

The following section presents the results from the centrifuge modelling of the building response to tunnelling.

2.1. Experimental setup

A series of centrifuge tests was carried out on the 8-m-diameter centrifuge at the University of Cambridge to investigate the response of buildings to tunnelling in sand. Centrifuge tests were carried out under plane strain conditions at 75g (Farrell, 2011). Using common scaling laws (Taylor, 1995), the model was designed to represent a tunnel with a diameter (D) of 6.15 m with a cover (C) of 8.25 m (at prototype scale), in fraction E silica sand. The model dimensions are shown in Fig. 2.

Sand was poured into the model to a relative density of 90% using an automatic sand pourer which enabled a high level of repeatability between tests. The model tunnel was formed using a brass mandrill with an outer latex rubber lining. The resulting annulus between the two was filled with water until an 82-mm-diameter cylinder was obtained. This model tunnel was then placed in a recess in the front Perspex face and the back aluminium plate to achieve plane strain conditions. During the test, volume losses were imposed by withdrawing the fluid from the tunnel using a piston and motor driven actuator system. Soil and building displacements at the Perspex face of the model were measured at incremental volume losses of 0.1%, using particle image velocimetry (PIV) (White et al., 2003). Physical displacement measurement instruments were also utilised to validate the PIV readings. Similar modelling techniques have been adopted by Taylor and

Grant (1998) and Marshall (2009) in the centrifuge modelling of the response to tunnelling of structures and pipelines, respectively. Further details of the modelling system are presented by Farrell and Mair (2011). Shibayama et al. (2010) presented the results of centrifuge tests investigating the response of sand to tunnelling, while Cui and Kimura (2010) provided a summary of a similar centrifuge modelling of a tunnel excavation.

2.2. Modelling of buildings

Two different types of idealised model buildings were considered in this study, namely, fully elastic beam structures and beam structures capable of cracking. The fully elastic structures used in this series of tests were constructed from aluminium beams ($E=70$ GPa) of varying thicknesses. The width of each aluminium beam was kept constant throughout the test series ($B=400$ mm) and each structure was placed symmetrically about the tunnel axis. In each case, plane strain conditions were present. A rough interface was modelled by gluing fraction E sand to the base of the structure. Geometric and structural properties for each of the 4 aluminium test beams (STR-1 to STR-4) are given in Table 1 and illustrated in Fig. 3.

Beam buildings, capable of cracking, were also modelled using micro concrete and masonry with cement-based mortar. Micro concrete mixes were formed from Ordinary Portland Cement (OPC) and various grades of relatively fine sand. The stiffness of the mix at various water–cement ratios (w/c) was calibrated using point load tests on sacrificial model beams. This also allowed for the effect of time on the strength of the mix to be assessed.

Masonry buildings were modelled using 1/12th scale model bricks with an OPC-based mortar. A further masonry building, termed MAS-2R, was modelled using 1/50th scale model bricks with an elastic silica gel mortar to simulate a beam with very low bending and axial stiffness. The geometric and structural properties for each of the beams tested are given in Table 1. All of the masonry buildings were located with an eccentricity (e) such that the building centreline was offset from the tunnel centreline. Farrell and Mair (2011) have also demonstrated that the range in prototype scale axial (EA) and bending (EI) stiffness values are comparable to those from similar centrifuge studies and from estimates of the stiffness of actual buildings from case studies. Assuming a uniform distribution under the footing, prototype scale modelled bearing pressure levels, exerted on the ground, varied between 5 and 50 kPa. No additional loading was applied to the buildings.

2.3. Building settlements

The settlement profiles of the aluminium beam buildings, STR-1 to STR-4, at a 2% volume loss are illustrated in Fig. 4. The greenfield settlement profile (GF-1) is also shown for reference. STR-1 is seen to behave fully flexibly with regions of hogging and sagging evident, while STR-4 demonstrates the most rigid response. Therefore, depending on a building's stiffness, or more specifically, ρ^*_{mod}, the settlement response can be fully flexible, fully rigid, or somewhere in between. Clearly, a more rigid response implies smaller distortions and strains, and consequently, less damage. This highlights the fact that assuming a building follows the greenfield settlement is potentially conservative.

The settlement response of STR-4 clearly indicates that the edges of the building settle more than the greenfield trough and 'embed' into the soil. Above the tunnel centreline, however, building settlements are substantially less than the greenfield values, suggesting the formation of a gap between the soil and the building. The development of a gap beneath buildings STR-2 to STR-4 has been confirmed from PIV measurements and stress cells (Farrell, 2011), and indicates that the building weight is redistributed towards the building edges causing settlements to be greater than the greenfield values in that region.

The settlement profiles of the micro concrete and masonry buildings in tests MCS-1, MAS-1, and MAS-2, at a 2% volume loss, are illustrated in Fig. 5a–c, respectively. The settlement profile of the ground beneath the buildings is also illustrated.

Table 1
Test series details.

Test name	Material	Model scale						Prototype scale	
		B (mm)	e[a] (mm)	t (mm)	L (mm)	EI (kNm^2/m)	EA (kN/m)	EI (kNm^2/m)	EA (kN/m)
GF-1					Greenfield—no building				
STR-1	Aluminium	400	0	1.6	145	2.4×10^{-2}	1.1×10^{5}	1×10^{2}	8.4×10^{6}
STR-2	Aluminium	400	0	5	145	7.3×10^{-1}	3.5×10^{5}	3.1×10^{5}	2.6×10^{4}
STR-3	Aluminium	400	0	10	145	5.8×10^{0}	7×10^{5}	2.5×10^{6}	5.3×10^{7}
STR-4	Aluminium	400	0	20	145	4.7×10^{1}	1.4×10^{6}	2.0×10^{7}	1.0×10^{8}
MCS-1	Micro-concrete	400	0	5	145	4.1×10^{-2}	2.0×10^{4}	1.8×10^{4}	1.5×10^{6}
MAS-1	Masonry	115	−67	10	18	1.6×10^{-1}	2.0×10^{4}	7.1×10^{4}	1.5×10^{6}
MAS-2	(a) Masonry[b]	195	−45	10	18	1.25×10^{-1}	1.5×10^{4}	5.4×10^{4}	1.1×10^{6}
MAS-2	(b) Masonry[b]	75	120	10	5	1.25×10^{-2}	1.5×10^{3}	5.4×10^{3}	1.1×10^{5}

[a]Where, e is the eccentricity of the building measured as the distance from the mid-point of the building to the tunnel centreline.

[b]Two buildings were tested in MAS-2. Building (a), MAS-2L, was located to the left of the tunnel centreline and building (b), MAS-2R, was located to the right of it.

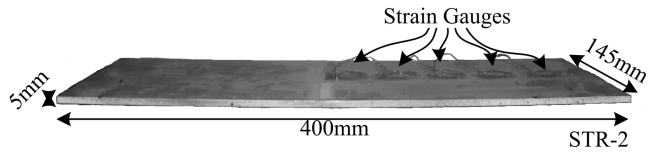

Fig. 3. Model aluminium beam building (STR-2) with strain gauges.

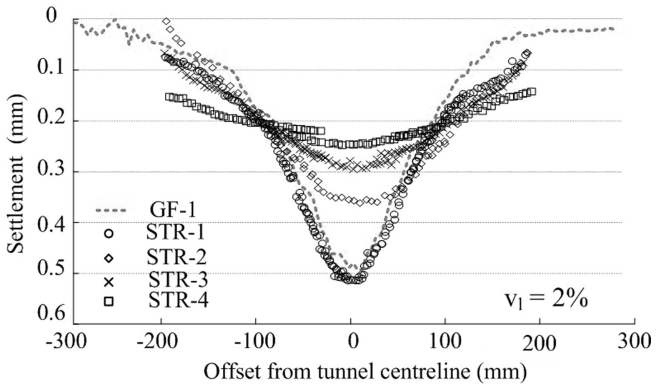

Fig. 4. Settlement profile for structures STR-1 to STR-4.

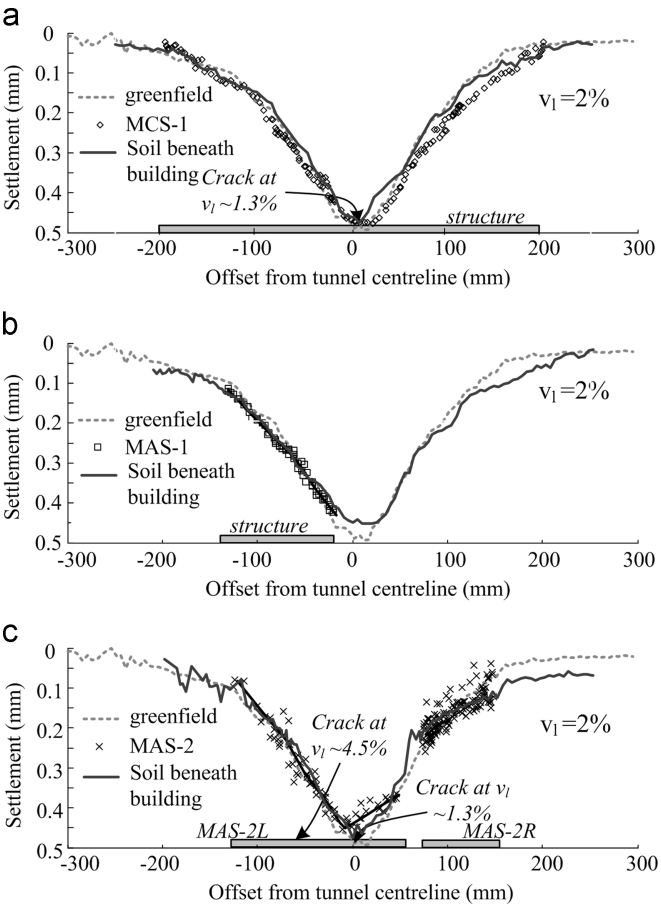

Fig. 5. Building settlements compared with greenfield settlements in tests (a) MCS-1, (b) MAS-1, and (c) MAS-2.

Building MCS-1 is seen to respond relatively flexibly, with regions of hogging and sagging evident. MAS-1, on the other hand, was observed to behave relatively rigidly and simply

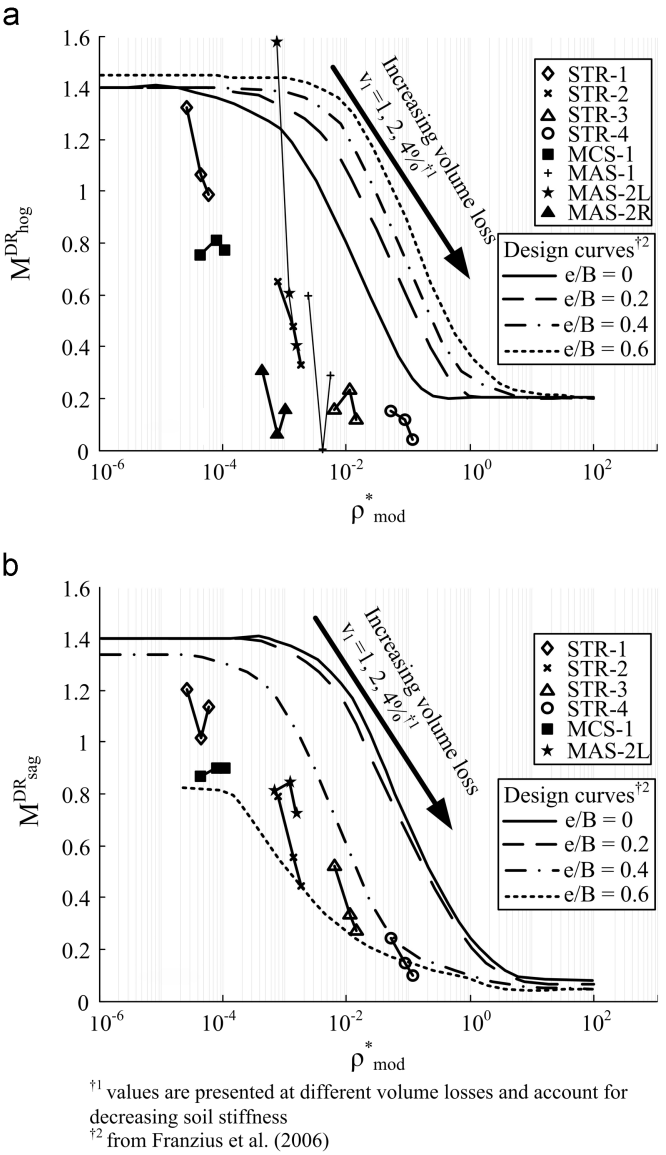

†1 values are presented at different volume losses and account for decreasing soil stiffness
†2 from Franzius et al. (2006)

Fig. 6. Modification factors in (a) hogging and (b) sagging (from Franzius et al., 2006).

tilted. The response of MAS-2L was found to be relatively flexible, with both hogging and sagging modes of deformation observable, although the response is significantly influenced by the development of a crack above the tunnel centreline. Scatter in the settlement data for MAS-2R is observed, although the response appears to be relatively flexible.

2.4. Modification to settlement distortions

The observed relationship between modification factors to the settlement distortions and the relative building stiffness defined by Franzius et al. (2006) (ρ^*_{mod}) is shown in Fig. 6a and b for hogging and sagging distortions, respectively. Design curves proposed by Franzius et al. (2006) are also shown. Measured modification factors are presented at volume losses of 1, 2, and 4% and account for the effect of changes in the soil stiffness on ρ^*_{mod}. The increase in volume loss generally leads to a

progressive reduction in soil stiffness (due to the increasing shear strain), and therefore, an increase in ρ^*_{mod}. The relationship between soil stiffness and strain was determined from a series of triaxial compression tests. An interesting observation is that for the very flexible STR-1, modification factors greater than unity are observed. This is consistent with observations from finite element analyses (Franzius et al., 2006) and indicates that the distortions are larger than the greenfield values. This is likely to result from the influence of horizontal shear stresses acting at the base of the building to increase the curvature.

The relationship between ρ^*_{mod} and M^{DR} is seen to be highly non-linear in both hogging and sagging, which again is in agreement with observations from the finite element analyses by Franzius et al. (2006). This highly non-linear relationship is highlighted by the decrease in M^{DR} for the elastic beams (STR-1 to STR-4) as volume losses increase. This decrease in M^{DR} arises as volume losses increase the soil strains which, in turn, reduces the soil stiffness, increases ρ^*_{mod}, and results in an increasingly rigid response. This trend is not as evident for non-elastic buildings, as cracking simultaneously reduces the building stiffness and ρ^*_{mod}. Note that scatter in the measured modification factors arises due to the precision of the PIV measurement system.

While the agreement between the design lines and the measured M^{DR} values is relatively poor, the design lines do represent an upper bound to the modification factors, as was their intended purpose. Scatter in the modification factors – as exemplified by MAS-2L in hogging – results from the limits of the precision (0.02 mm) of PIV and the ensuing errors in estimating the deflection ratio.

2.5. Horizontal displacements and strains

Fig. 7a–c show the horizontal displacement profile of buildings STR-4, MAS-1, and MAS-2, respectively, at a 2% volume loss. Greenfield horizontal displacements are also illustrated for reference. It can be observed that STR-4 displayed negligible horizontal displacements and significantly modified the greenfield displacement profile. All buildings placed symmetrically about the tunnel centreline displayed similar behaviour; this is to be expected, as there would be zero horizontal displacement for a building symmetrically placed about the tunnel centreline.

Building MAS-1, on the other hand, displays a net horizontal displacement which is roughly equal to the maximum greenfield horizontal displacement, indicating that the ground laterally displaces the building. Differential horizontal displacements, and hence, horizontal strains, however, remain negligible. A net horizontal displacement of building MAS-2L (see Fig. 7c) is also observed, although the magnitude of this displacement is less than the maximum greenfield displacement. Horizontal displacements of building MAS-2R are seen to agree reasonably well with the greenfield values.

Horizontal displacements of the buildings and the soil surface – illustrated by the solid black line – in test MAS-2 at a volume loss of 2% are presented in more detail in Fig. 8. Greenfield horizontal displacements are presented for reference. Horizontal strains,

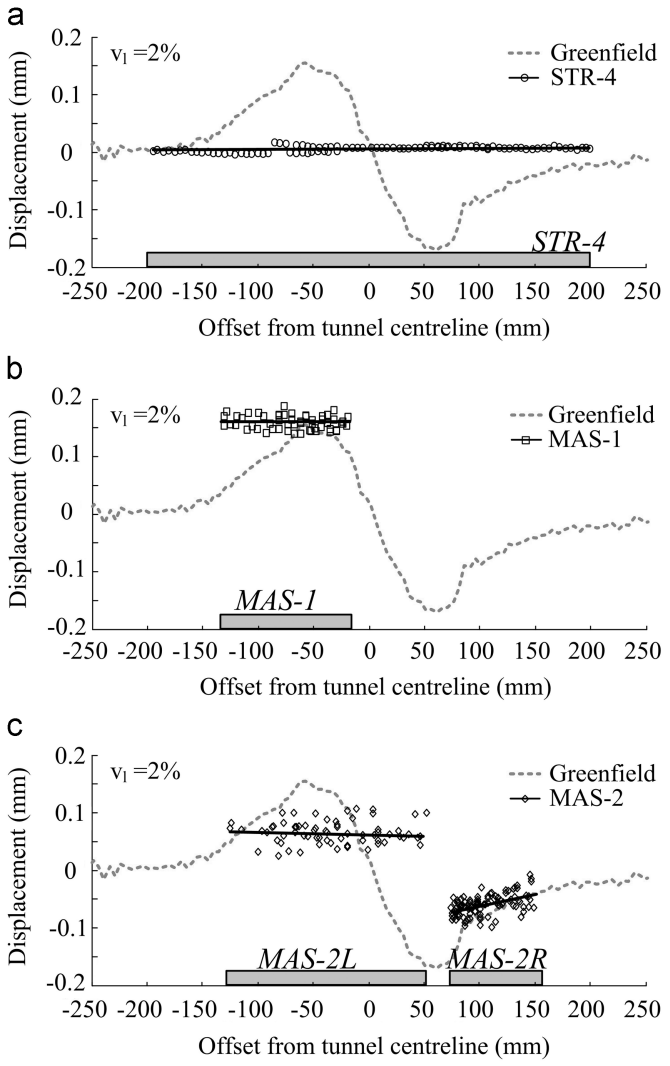

Fig. 7. Horizontal displacement profile for model buildings in tests (a) STR-4, (b) MAS-1, and (c) MAS-2.

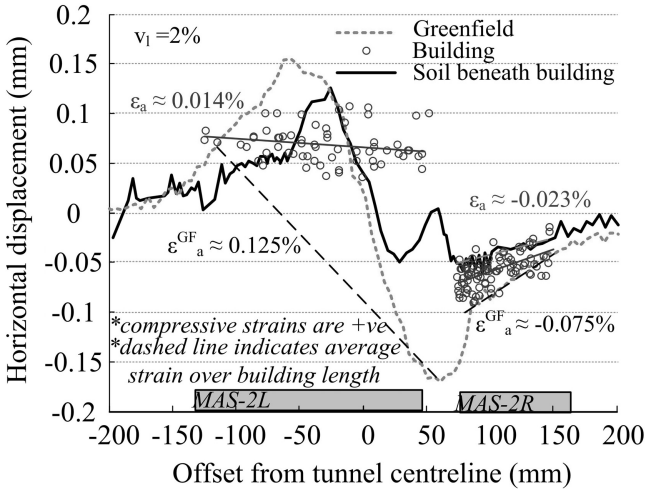

Fig. 8. Estimation of horizontal strains from measured horizontal displacements of buildings in test MAS-2 and from greenfield measurements.

estimated from the slope of a straight line fitted to the horizontal displacements, are also indicated. MAS-2L can be seen to restrain horizontal displacements towards its edges. This is particularly evident towards the right-hand side of the building ($x \sim 60$ m) where large greenfield horizontal displacements (~ 0.2 m) are reduced to almost zero. The better agreement between the measured horizontal displacements and the greenfield displacements close to the tunnel centreline (e.g., $x \sim -40$ mm), indicate that friction in this region is significantly lower than at the edges. This is consistent with the potential formation of a gap between the soil and the building above the tunnel centreline and would explain the net horizontal displacement of the building towards the tunnel centreline.

Average greenfield horizontal strains across building MAS-2L can be estimated as 0.125%, where compression is positive, as illustrated by the dashed black line. Although there is some scatter in the data, horizontal strains within MAS-2L are substantially smaller and are approximately 10% of the greenfield values. A comparison of horizontal displacements in the ground directly beneath the building, with those of the building itself, indicates that the horizontal ground strains, while significantly smaller than the greenfield values, are larger than those in the building. This demonstrates how the soil-structure interaction also modifies the displacements and strains in the soil beneath the building.

Horizontal strains within MAS-2R, however, are evident from the differential horizontal displacements. They are around 30% of the average greenfield horizontal strain. The prototype scale axial stiffness (EA) of this building, however, is extremely low, due to the silica gel mortar and is equivalent to only a 4-mm-thick reinforced concrete slab (for $E=27$ GPa). Horizontal strains within the aluminium beams tested were also found to be negligible relative to greenfield strains. Similar conclusions of negligible horizontal strains being induced in buildings with continuous footings have been reached by Viggiani and Standing (2001), Mair (2003) and Dimmock and Mair (2008).

3. A case study in Bologna

A 12-m-diameter tunnel was constructed beneath two buildings using the sprayed concrete lining (SCL) method and extensive protective measures. The tunnel axis is located at 20.95 mAD and the ground level varies from 44.3 to 46.2 mAD, giving a minimum depth of cover (C) of about 17.3 m. A plan of the site is presented in Fig. 9, which also details the extensive instrumentation adopted to monitor the tunnelling works. Construction was carried out from east to west in 6-m stages, with the exception of the first stage, which was 12 m in length. Further details of the protective measures, which consisted of both vertical and horizontal jet grouting, amongst other methods (including drains and piles), are presented in detail by Farrell et al. (2011) and Farrell (2011). Jet grouting from the surface was carried out from stages 1 to 4, while horizontal jet grouting from within the tunnel was carried out between stages 4 and 18.

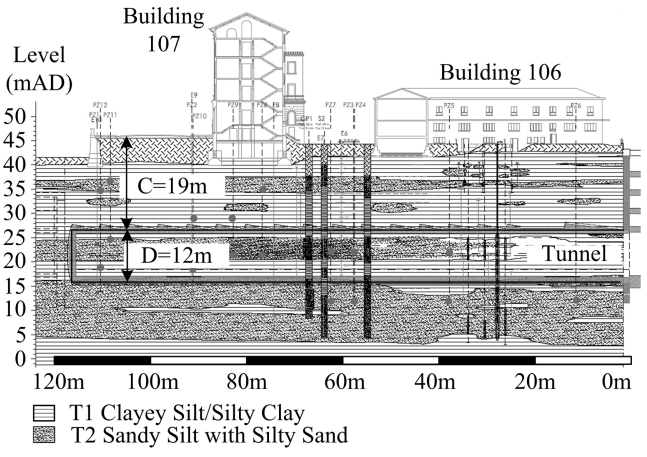

Fig. 10. Elevation of site and stratigraphy.

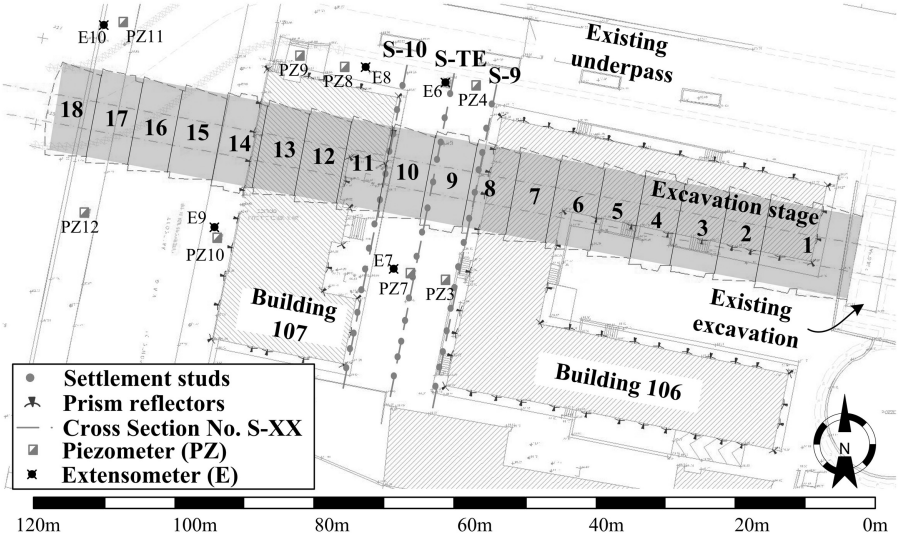

Fig. 9. Site plan.

3.1. Ground conditions

The site geology consists of over-consolidated fluvial deposits from the Quaternary period. Ground conditions, illustrated in Fig. 10, are highly stratified with layers of silty clays and clayey silts, termed the T1 formation, interbedded with lenses of sandy silt and silty sand, termed the T2 formation. These descriptions have been confirmed from particle size distribution tests. Casagrande plasticity charts classify the T1 formation as a medium to high plasticity clay.

The water table was found to lie 5 m below ground level (~39 mAD), although under-drainage from an underlying gravel layer means that conditions are not hydrostatic. The permeability of the T2 formation beneath the tunnel invert was estimated from in-situ permeability tests to lie between 10^{-6} to 10^{-7} m/s. The high fines content of the T1 formation (72–99%) indicates a very low permeability; this is consistent with the observed lack of water inflows at the tunnel face throughout construction.

Results from CPT tests indicate that the undrained shear strength (c_u) at the tunnel axis was around 120 kPa. SPT and undrained unconsolidated (UU) triaxial tests indicate lower strengths of around 80 kPa, although this may be due to sample disturbance.

Correlations proposed by Duncan and Buchignani (1976) are used to estimate the undrained soil stiffness (E_u) from the undrained shear strength, taking $E_u = 600\ c_u$, for $I_p = 30\%$. Based on these correlations, E_u at a depth of $z = z_0/2$ is estimated to be about 90 MPa.

3.2. Greenfield settlements

For the purpose of investigating greenfield ground movements, cross section S-TE (see Fig. 9) is analysed as it is the least influenced by the adjacent buildings. Fig. 11 shows the settlement profile along section S-TE at various stages during the excavation. Gaussian curves fitted to the settlement data are also illustrated. Settlements can be seen to increase as the tunnel face proceeds towards the cross section. As the tunnel face passes beyond section S-TE ($d > 0$), the contribution of further construction to the maximum settlement (196 mm) can be seen to be relatively small, indicating that most of the settlement occurs ahead of the tunnel face.

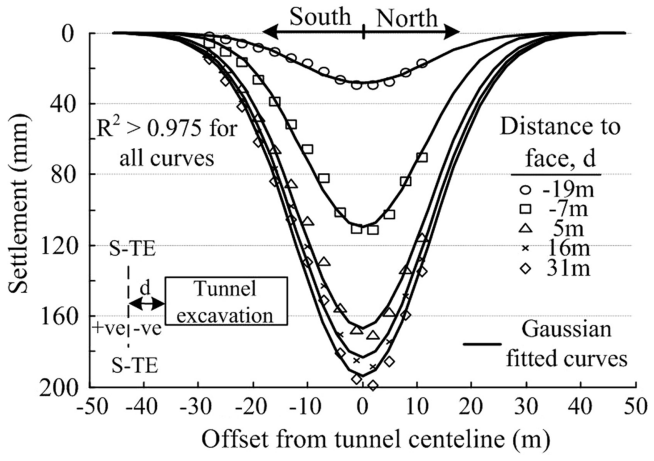

Fig. 11. Greenfield surface settlement profile at section S-TE.

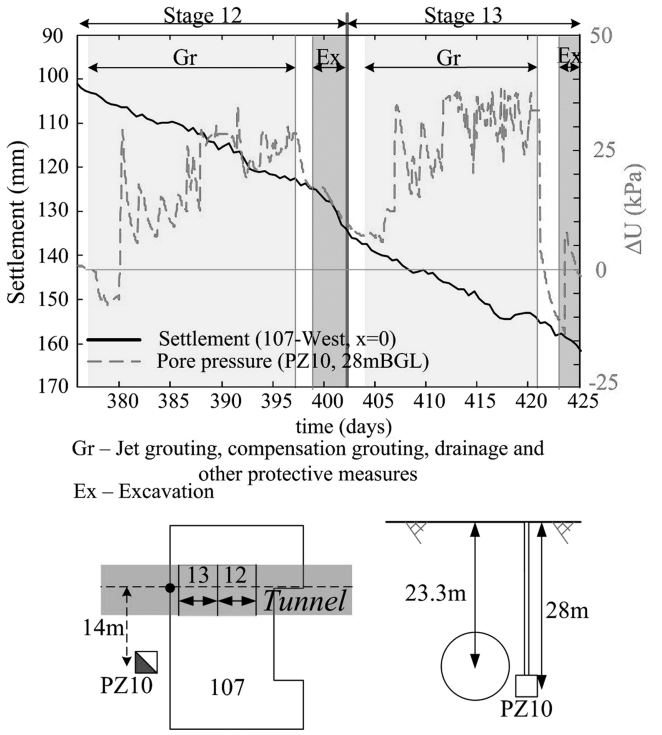

Fig. 12. Variation in pore pressure and settlement during construction of stages 12 and 13.

From the area of the settlement trough, expressed as a percentage of the cross-sectional tunnel area, volume losses at section S-TE can be estimated as 5.1%, assuming negligible contraction or dilation of the soil and ignoring the effects of consolidation. Bearing in mind that typical volume losses for open-face tunnelling in stiff clay are in the range 1.0–2.0% (Mair and Taylor, 1997), this is a large volume loss for an urban tunnelling project. These volume losses are addressed briefly in Section 3.3 and are discussed further by Farrell et al. (2011). Nonetheless, Farrell (2011) has demonstrated that the volume losses occurring after horizontal jet grouting commenced (see Fig. 9 for grouting location details) remain relatively consistent.

3.3. Causes of volume losses

Despite the extensive protective measures adopted during this project, large volume losses have been observed, particularly where horizontal jet grouting was carried out from within the tunnel excavation alone, as was the case beneath section S-TE.

Fig. 12 shows the settlement response of the western façade of building 107 at the tunnel centreline ($x = 0$) against time during stages 12 and 13 of the excavation (indicated in Fig. 12). The change in pore pressure (ΔU) against time, measured just below the tunnel axis (28 mbgl) by piezometer

PZ10, is also shown. Pore pressure changes are related to the measurements at the time of installation of the piezometer. This occurred when the perpendicular distance from the tunnel face to the piezometer was around 20 m. The jet grouting is observed to cause a large increase in pore pressure which is consistent with an undrained response of the ground, as highlighted by Mair and Taylor (1993).

A large increase in settlement is observed during the jet grouting in stage 12, while the tunnel excavation itself causes only a slight increase in the settlement rate. Subsequent jet grouting during stage 13 is observed to coincide with further increasing settlements of building 107. Again, the excavation of section 13 does not appear to have a significant impact on the rate of settlements. In total, up to 70% of the building settlements occurred during phases of horizontal jet grouting. The effects of consolidation, and the tunnel excavation itself, also contributed to the settlements. It is clear that the protective measures adopted, although necessary to ensure tunnel stability, contributed significantly to the observed settlements.

3.4. Building details

Two buildings overlie the excavation, both of which have been constructed with load bearing masonry walls on strip footings with reinforced concrete floor slabs. The building to the west of the site, building 107, is a 5-storey commercial structure. The building to the east of the site, building 106, is a 2-storey structure. Both buildings lie transverse to the tunnel axis, and the eccentricity, defined as the distance from the midpoint of the building to the tunnel centreline, is 8.7 m ($e/B=0.23$).

The bending stiffness (EI) of buildings 106 and 107 has been estimated by summing the individual stiffness of each structural component, including walls, slabs, and footings (see Eq. (4)). As the buildings are constructed from load-bearing masonry, it is assumed that shear transfer between the walls and the slabs is negligible. Consequently, the neutral axis of each component is taken to be about that of the individual member itself. The stiffness of all components is reduced to per metre length values in the plane of bending. E values for the load-bearing masonry and the reinforced concrete are taken as 3×10^6 kN/m^2 and 27×10^6 kN/m^2, respectively. Dimmock and Mair (2008) have demonstrated the importance of accounting for the effect of openings on the building stiffness. These effects are accounted for by applying the reduction factors, proposed by Melis and Rodriguez Otiz (2001), to the EI values for walls.

$$EI_{building}=\sum EI_{walls}+\sum EI_{slabs}+\sum EI_{footings} \quad (4)$$

Using this approach, the bending stiffness for the western section of building 106 in the plane transverse to the tunnel heading was estimated as 4.9×10^6 kNm^2/m. EI for building 107 was estimated to be almost two orders of magnitude larger, at 2.3×10^8 kNm^2/m. For both buildings the internal and external walls were found to contribute to the majority of the bending stiffness. By summing the axial stiffness of each component in a similar manner to that outlined above, EA values for buildings 106 and 107 have been estimated as 9.3×10^6 kN/m and 2.5×10^7 kN/m, respectively.

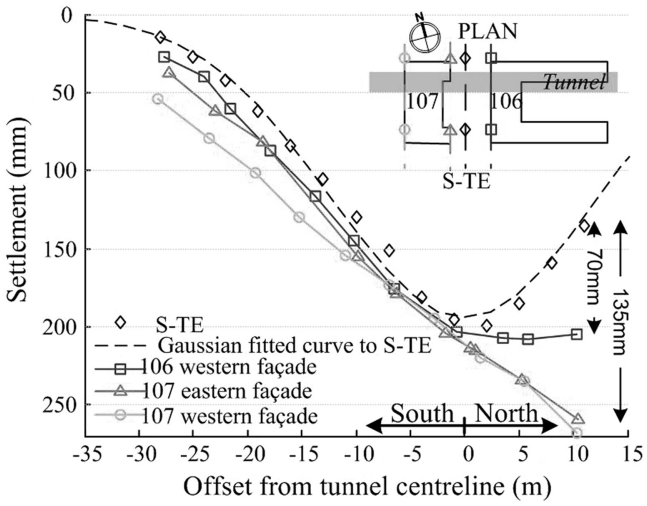

Fig. 13. Building and greenfield settlement profiles.

The relative bending stiffness, ρ^*_{mod}, has been estimated for buildings 106 and 107 to be 6.7×10^{-2} and 3.5×10^{0}, respectively. Note that for each case, z_0 has been adjusted to account for the foundation depth, and the soil stiffness (E_s) has been taken as 90 MPa.

3.5. Building settlement response

Observed settlements of the western façade of building 106, the eastern and western façades of building 107, and the greenfield section S-TE are illustrated in Fig. 13. It is apparent that building 107 responded rigidly and simply tilted towards the tunnel centreline with no distinct hogging or sagging regions observable. This tilt response is observed to result in settlements at the northern edge ($x=10$ m) that are significantly larger (265 mm) than the equivalent greenfield settlements (130 mm). Settlements of building 107, around the trough shoulders, are also larger than the greenfield values, indicating that the building embeds into the soil. This embedment is likely to have resulted from a redistribution of the building weight as the tunnel excavation progressed towards the building and is similar to that observed from centrifuge modelling in Fig. 4. Similar observations of building tilt towards the tunnel centreline have been made by Sung et al. (2006).

In contrast to building 107, the response of building 106 is seen to be relatively flexible with clear regions of hogging and sagging. Slight modification to the greenfield settlement profile can be seen, particularly towards the north of the building ($x>0$ m) where, similar to building 107, settlements (200 mm) are larger than the equivalent greenfield values (130 mm). This embedment of the building is probably also due to the redistribution of the building weight as the excavation progressed beneath the building. However, as building 106 behaved relatively flexibly, this redistribution is not as significant as for building 107. The lower weight of

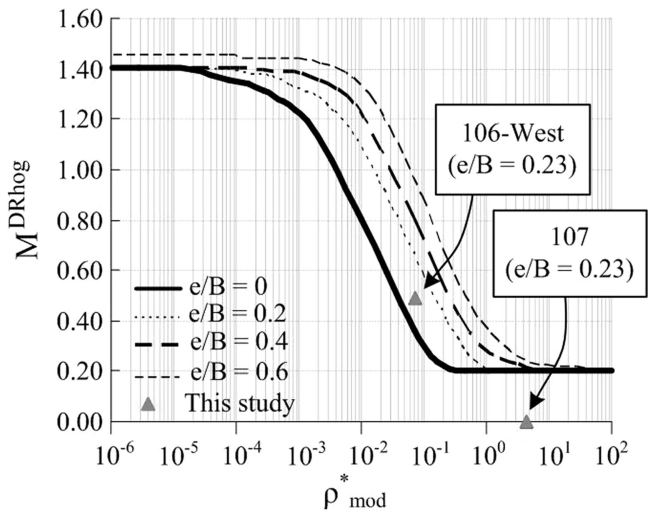

Fig. 14. Modification factors versus relative building stiffness for buildings in sagging with design lines (from Franzius et al., 2006).

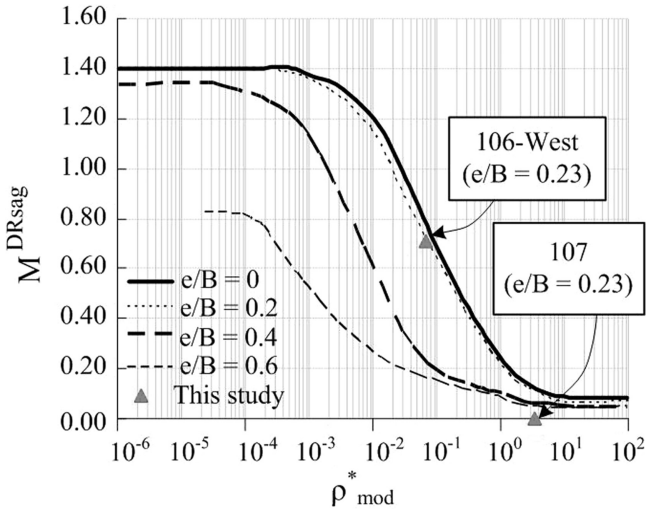

Fig. 15. Modification factors versus relative building stiffness for buildings in hogging with design lines (from Franzius et al., 2006).

building 106, relative to 107, may also explain why the embedment of building 106 is smaller although, as discussed in Section 2.4 and below, the modification to the greenfield settlement profile is governed by the relative soil–structure stiffness.

Building embedment has been verified from extensometer readings taken 3 m to the north of building 107, where settlements were comparable with greenfield measurements (see Farrell et al., 2011). This also indicates that, as with the conclusions from centrifuge modelling, greenfield settlements are restored within a relatively short distance from the building—in some cases, there is a potential concern for the adjoining infrastructure. While finite element models have identified trends of building embedment into the soil, buildings have generally been modelled as weightless beams; and thus, an important aspect of the soil structure interaction is perhaps missing.

The effect of a building's weight on its response to tunnelling has been investigated through finite element modelling by Franzius et al. (2004). Whilst the weight affected the response, results demonstrated that it was the relative soil–structure stiffness that predominately governed the response. Although not addressed fully in this paper, Farrell (2011) came to a similar conclusion based on results from centrifuge modelling. Similar to Franzius et al. (2004), Shahin et al. (2011) demonstrated that building loads influence the magnitude of the settlements caused by tunnelling, although this is beyond the scope of the present paper.

3.6. Quantifying soil structure interaction

Fig. 14 illustrates the relationship between the measured deflection ratios of buildings 106 and 107 (from the settlement profiles illustrated in Fig. 13) and the relative building stiffness. Values for DR^{GF} after construction are determined from cross section S-TE and have been calculated to be 0.13 and 0.27 in hogging and sagging, respectively. Due to the rigid response of building 107, DR^{str} values and corresponding modification factors equal zero in both hogging and sagging. DR^{str} values for the western façade of buildings 106 are calculated as 0.06 and 0.19 in hogging and sagging, respectively. Corresponding modification factors for building 106 are 0.46 and 0.7, respectively. These modification factors indicate that building 106 responded more flexibly in sagging than in hogging. This is contrary to evidence in the literature which suggests that buildings behave more flexibly in hogging due to the inability of masonry walls to sustain tensile strains near the roof and the reinforcement provided by the foundations in sagging (Burland and Wroth, 1974; Mair, 2003). For the case of building 106, however, the foundations are not reinforced which may explain this observation. Farrell (2011) has also demonstrated that the length of the building within the sagging region, being longer than that in the hogging region, has a significant effect on the increased flexibility of the sagging region.

Upper bound design lines, which relate M^{DR}, in both hogging and sagging, to the relative soil structure stiffness (ρ^{*}_{mod}), have been proposed by Franzius et al. (2006), as illustrated in Figs. 14 and 15, respectively. As with the results from centrifuge modelling in Fig. 6, design lines, for $e/B=0.2$, are found to provide an upper bound to the measured modification factors. The increased flexibility of building 106 in sagging is also predicted from the design lines, indicating that the building response to tunnelling is also a function of its location relative to the settlement trough. Goh (2010) has since refined the relative soil stiffness parameter to account for this variable and has demonstrated a clear reduction in scatter of the data.

4. Building damage assessments

Current damage assessment methods, such as that proposed by Mair et al. (1996), involve superimposing greenfield ground distortions, both vertical and horizontal, onto a building which is modelled as a simple beam (Burland and Wroth, 1974). Results from centrifuge modelling, however, have

Fig. 16. Cracking along western façade of building 106 (Borgonovo et al., 2007).

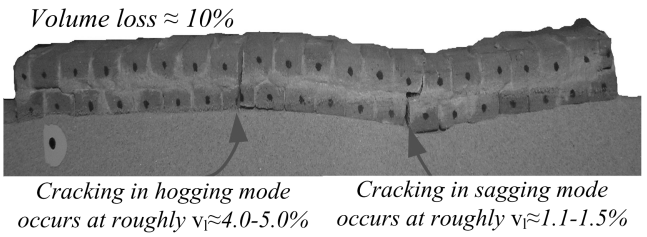

Fig. 17. Observed cracking of building MAS-2L in centrifuge testing.

demonstrated that the modification to the greenfield settlement distortions displayed by buildings can vary from zero to over 1 (see Fig. 6), while Fig. 8 suggests that horizontal strains are generally negligible, with the exception of buildings with an unrealistically low axial stiffness. Assuming buildings to deform fully flexibly by the same amount as the greenfield ground movements, can result in misleading estimates of the level of damage that will be caused.

In the Bologna case study, the horizontal response of buildings 106 and 107 was complicated by the protective measures adopted; however, Farrell (2011) demonstrated that the horizontal strains were less than 30% of the greenfield values. Therefore, as building 107 responded rigidly and simply tilted, the majority of damage to the building could be attributed to horizontal and twisting distortions. Due to the relatively small distortions, building 107 displayed only minor cracking of the internal plastering. Cracking of the external façade was minimal and the maximum crack width was measured as 1.1 mm. No significant damage was observed and, as a result, the level of damage can be classified as 'Very Slight to Slight' (as defined by Burland et al., 1977). In contrast, in the case of building 106, the large settlement distortions resulted in the jamming of doors and windows and severe cracking, particularly in hogging (see Fig. 16), although cracking was also observed in the sagging region. Significant re-pointing of the brickwork was also required, corresponding to a category 3 or 'Moderate' level of damage, as defined by Burland et al. (1977).

An assessment of the risk of damage to buildings 106 and 107 using the simple beam theory proposed by Burland and Wroth (1974), suggests that, had the buildings been subjected to greenfield distortions, the damage in both cases would have been in the 'Severe to Very Severe' category. This is clearly a significant overestimation of the risk of damage to both buildings and highlights the importance of considering the soil–structure interaction when estimating tunnelling-induced damage.

Furthermore, while current design approaches focus on the risk of damage to buildings in hogging, damage to non-elastic buildings, MCS-1 and MAS-2L in the centrifuge modelling, was initially observed in the sagging region of the trough, as tensile strains in the bottom fibre were not reduced by the greenfield horizontal compressive strains (see Fig. 17). This indicates that, while hogging induced distortions remain a significant concern, as demonstrated in the literature and in the Bologna case study, damage to buildings in the sagging region of the trough should also be considered.

5. Conclusions

Mechanisms governing the response of buildings to tunnelling have been investigated using results from both centrifuge modelling and a case study in Bologna. A good agreement between the mechanisms identified in each study was observed. The following conclusions can be made:

1. The modification to settlement distortions is a function of both the building and the soil stiffness, in addition to the geometric parameters. Estimated modification factors, using design charts proposed by Franzius et al. (2006), were found to provide upper bounds to the measured values. This shows that the design charts can be reasonably applied to practical tunnelling projects.
2. Horizontal ground strains, transferred into model buildings, were found to be negligible unless the prototype scale axial stiffness was unrealistically small for a building with continuous footings. Similarly, horizontal building strains in the Bologna case study were less than 30% of the greenfield values, although this was complicated by the grouting measures adopted. This is consistent with what has been observed in the field (Mair, 2003; Viggiani and Standing, 2001).
3. Assessing the risk of damage based on the assumption that buildings distort fully flexibly, conforming to the greenfield settlement and horizontal profiles, can be highly conservative. This may result in decisions regarding the need for protective measures (such as compensation grouting) being made on the basis of misleading damage estimates or, of less consequence, in unnecessary additional costs being incurred for finite element modelling.
4. Both centrifuge modelling and field data indicate that the redistribution of building weight due to tunnelling can significantly influence both the response of the building itself and of the subsoil. Rigid buildings tend to redistribute their weight and embed into the soil, while flexible

buildings simply deform according to the greenfield settlement profile. As the greenfield settlement profile is restored within a short distance from the building, in some cases this may have an impact on an adjoining infrastructure.

5. Damage to buildings in the hogging mode of deformation has generally been the primary concern of engineers assessing tunnelling-induced damage. The initiation of cracking in non-elastic buildings in centrifuge modelling, however, indicates that distortions in the sagging region should also be of concern. This arises from the lack of horizontal compressive strains mobilised in the building, which would otherwise negate the bending-induced tensile strains; this effect was observed in both centrifuge modelling and the Bologna case study.

References

Borgonovo, G., Contini, A., Locatelli, L., Perolo, M., Ramelli, E (2007) Monitoring used as an alarm system in tunnelling. In: Rapid Excavation and Tunnelling Conference Proceedings, 381-395.

Burland, J.B., Broms, B.B., De Mello, V.F.B. (1977). Behaviour of foundations and structures. In: Proceedings of the Ninth International Conference on Soil Mechanics and Foundations Engineering, 2, 495–546. Tokyo.

Burland, J.B., Wroth, C.P., 1974. Settlement of Buildings and Associated Damage. Settlement of Structures, Cambridge. Pentech Press, London, Cambridge611–654.

Cui, Y., Kimura, M., 2010. Model test and numerical analysis methods in tunnel excavation problem. Soils Found. 50 (6), 915–923.

Duncan, M.J., Buchignani, A.L., 1976. An Engineering Manual for Settlement Studies. University of California, Berkley.

Dimmock, P.S., Mair, R.J., 2008. Effect of building stiffness on tunnelling-induced ground movement. Tunnelling Underground Space Technol. 23 (4), 438–450.

Farrell, R.P., 2011. Tunnelling in Sands and the Response of Buildings. University of Cambridge (PhD Thesis).

Farrell, R.P., Mair, R.J., Sciotti, A., Pigorini, A., Ricci, M. (2011). The response of buildings to tunnelling: a case study. In: Proceedings of the Seventh International Symposium on Geotechnical Aspects of Underground Construction in Soft Clay, May, Rome.

Farrell, R.P., Mair, R.J. (2011). Centrifuge modelling of the response of buildings to tunnelling. In: Proceedings of the Seventh International Symposium on Geotechnical Aspects of Underground Construction in Soft Clay, May, Rome.

Franzius, J.N., Potts, D.M., Addenbrooke, T.I., Burland, J.B., 2004. The influence of building weight on tunnelling induced ground and building deformation. Soils Found. 44 (1), 25–38.

Franzius, J.N., Potts, D.M., Burland, J.B., 2006. The response of surface structures to tunnel construction. Proc. Inst. Civ. Eng. Geotech. Eng. 159 (1), 3–17.

Goh, K.H., 2010. Response of Ground and Buildings to Deep Excavations and Tunnelling. University of Cambridge, UK (Ph.D. Thesis).

Mair, R.J., Taylor, R.N. (1993). Prediction of clay behaviour around tunnels using plasticity solutions. In Predictive Soil Mechanics—Proceedings of the Wroth Memorial Symposium, pp. 449–463. Thomas Telford, Oxford, UK.

Mair, R.J., Taylor, R.N. (1997) Bored tunnelling in the urban environment. In: Proceedings. Forteenth International Conference on Soil Mechanics and Foundation Engineering. Hamburg. 4:2353–2385.

Mair, R.J., Taylor, R.N., Burland, J.B., 1996. Prediction of Ground Movements and Assessment of Risk of Building Damage Due to Bored Tunnelling. Geotechnical Aspects of Underground Construction in Soft Ground, 713–718 (Balkema, London).

Mair, R.J. (2003). Research on tunnelling-induced ground movements and their effects on buildings-lessons from the Jubilee Line Extension. Keynote Lecture, In: Proceedings of the International Conference on Response of Buildings to Excavation-induced Ground Movements, held at Imperial College London, UK, July 2001, pp. 3–26, Jardine F.M. (Eds.), CIRIA SP199.

Marshall, A.M., 2009. Tunnelling in Sand and its Effect on Pipelines and Piles. Engineering department, Cambridge University (PhD Thesis).

Melis, M.J., Rodriguez Otiz, J.M., 2001. Consideration of the stiffness of buildings in the estimation of subsidence damage by EPB tunnelling in the Madrid subway. In: International Conference on the Response of Buildings to Excavation Induced Ground Movements, 387–394 (CIRIA SP 201).

Potts, D.M., Addenbrooke, T.I., 1997. A structures influence on tunnelling induced ground movements. Proc. Inst. Civ. Eng. Geotech. Eng. 125, 109–125.

Shahin, F., Nakai, H.M., Zhang, M., Kilumoto, M., Nakahara, E., 2011. Behavior of ground and response of existing foundation due to tunneling. Soils Found. 51 (3), 395–409.

Shibayama, S., Izawa, J., Takahashi, A., Takemura, J., Kusakabe, O., 2010. Observed behavior of a tunnel in sand subjected to shear deformation in a centrifuge. Soils Found. 50 (2), 281–294.

Sung, E., Shahin, H.M., Nakai, T., Hinokio, M., Yamamoto, M., 2006. Ground behavior due to tunnel excavation with existing foundation. Soils Found. 46 (2), 189–207.

Taylor, R.N., 1995. Geotechnical Centrifuge Technology. Blackie Academic and Professional, London.

Taylor, R.N, Grant, R.J., 1998. Centrifuge modelling of the influence of surface structures on tunnelling induced ground movements. In: Negro, Jr, Ferreira (Eds.), Tunnels and Metropolises. Balkema, Rotterdam, pp. 261–265.

Viggiani, G., Standing, J.R., 2001. The treasury. In: Burland, J.B., Standing, J.R., Jardine, F.M. (Eds.), Building Response to Tunnelling: Case Studies from Construction of the Jubilee Line Extension, London, vol. 2. CIRIA and Thomas Telford, London, pp. 351–366.

White, D.J., Take, W.A., Bolton, M.D., 2003. Soil deformation measurement using particle image velocimetry (PIV) and photogrammetry. Geotechnique 53 (7), 619–631.